Non-invasive Early Detection of Acute Cardiac Allograft Rejection by MRI in Rodent Model

Y. L. WU[1], K. Sato[1], Y. Sun[2], H-H. Chang[2], K. Hitchens[1], J. Moura[2], C. Ho[1]

[1]Pittsburgh NMR Center for Biomedical Research, Carnegie Mellon University, Pittsburgh, PA, United States, [2]Electrical and Computer Engineering Department, Carnegie Mellon University, Pittsburgh, PA, United States

INTRODUCTION:

The goal of this study is to investigate functional parameters that can detect early cardiac allograft rejection non-invasively with MRI in order to supplement or potentially replace current gold standard for diagnosing rejection, biopsy, which is invasive and prone to sampling errors.

METHODS:

1. Animal model: We developed abdominal heterotopic working heart and lung transplantation model in rats using DA to BN combination.
2. MRI methods: Cine imaging was used to evaluate cardiac function. Tagging was achieved by a modified DANTE sequence.

RESULTS:

The abdominal heterotopic transplanted hearts exhibited similar cardiac function and output as well as ventricular pressure close to native hearts. Fig.1 shows cine and tagging images of a transplanted heart. Not until the severe rejection occurs, there is significant change detected in global systolic functions, such as ejection fraction. The goal of this study is to investigate functional parameters for early detection of rejection before irreversible heart damage occurs. We have explored the time-dependent characteristics of the left ventricular (LV) volume (LVV) and the LV wall motion in earlier rejection stages at post-operational day (POD) 3, 4, and 5, when mild to moderate rejection was manifested.

At early rejection stages, both allografts and isografts exhibited similar hemodynamic properties for LVV (Fig.2A). However, allografts showed slightly prolonged isovolumic relaxation phase. The relative isovolumic relaxation time span (T_{IVR}) for allografts increased over time as the rejection worsened (Fig. 2B). On the contrary, T_{IVR} for isografts shortened over time, as the grafts recovered from the ischemic injury of the transplantation operation. This is indicative that the diastolic dysfunction precedes systolic dysfunction and T_{IVR} is a sensitive non-invasive index for detecting the early changes in diastolic dysfunction resulting from acute rejection.

In addition to temporal behavior, the spatial properties of the transplanted hearts were investigated with tagging (Fig.4) and regional wall motion was analyzed by the centerline method (Fig.3). Figure 3 shows regional wall motion analysis for 2 isografts (Fig.3 A,B) and 2 allografts (Fig.3 C,D). 100 chords were placed across the LV wall and the chord length was measured at 10 phases in a cardiac cycle. Two phases, ES and ED, are shown. With no rejection (Fig.3 A,B), the LV wall thickened and shortened in a coordinated fashion throughout the entire LV wall with relatively homogeneous extent of thickening. On the other hand, the rejected allografts (Fig.3 C,D) showed inhomogeneous thickening and thinning at different parts of the LV wall. Moreover, different parts of the LV wall thickened and shortened at different time in an asynchronous manner. The spatial heterogeneity in contractility can be easily seen with tagging (Fig. 4). The brightness of the strain map (Fig.4 A, B) represents the extent of stretching. The angle and the extent of the twist and radial shortening (Fig. 4 C, D) are represented by the direction and the length of the arrow heads at each intersection of tag lines. For this particular heart, the inferolateral (upper left) and anterior (lower right) LV wall preserved most of the motility whereas the anterolateral wall (lower left) has lost its contractility.

CONCLUSIONS:

Our data suggest that diastolic dysfunction precedes systolic functional loss. The relative time span of the isovolumic relaxation, regional wall motion, and tagging are sensitive for detection early rejection, which can potentially be used for non-invasive diagnosis for early cardiac allograft rejection.

Fig.1

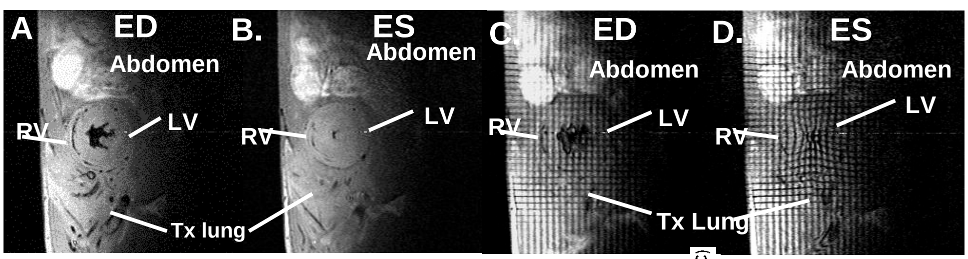

Fig.2

Fig.3

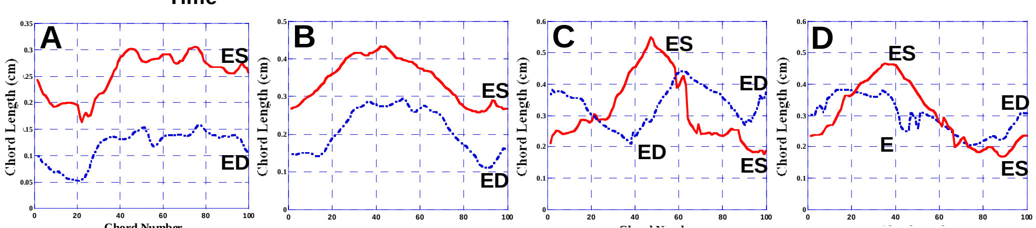

Fig.4